Benchmark of wrinkling formulae and methods for pre-sizing of aircraft lightweight sandwich structures

M. Ginot [a,c], M. D'Ottavio [b], O. Polit [b], C. Bouvet [c], B. Castanié [c,*]

[a] Elixir Aircraft, 3 Rue du Front de Mer, 17000La Rochelle, France
[b] LEME – EA4416, Université Paris Nanterre, 50, Rue de Sèvres, 92410 Ville d'Avray, France
[c] Institut Clément Ader (ICA), ISAE, CNRS, UMR 5312-INSA-Mines Albi-UPS, Toulouse, France

Keywords:
Sandwich structures
Wrinkling
Benchmark
Light aviation

A B S T R A C T

Sandwich structures are widely used in many industrial applications and especially in light aviation. The local buckling phenomenon named "wrinkling" is one of the primary causes of compressive failure of such structures. Its calculation is a difficult practical problem since this phenomenon cannot be captured by the GFEM (Global Finite Element Model) classically used for aircraft structure sizing. Therefore, pre-sizing involves the use of a wrinkling model, which can be found in the literature. In practice, such models are used with high safety factors by the industry. This paper proposes an evaluation of analytical wrinkling formulas in an industrial setting. Realistic applications involve a framework (3D stress state, orthotropy, skin asymmetry) far from the assumptions on which most of the analytical formulations are based. The case study is a sandwich composite beam subjected to uni-axial compressive load. Limitations and assumptions of the analytical wrinkling models studied are quantified and a discussion on the relevance of using simple formulas for the design of sandwich structured composites is developed.

1. Introduction

Sandwich structures consist of two thin, high-strength material skins that are separated by a thick, relatively weak, lightweight material, the core. The high specific bending stiffness renders sandwich structures attractive for load bearing design solutions with consistent weight savings. They have been widely used in aviation for more than a hundred years now [1]. However, they are mainly used for primary structures only in low carrying and non-pressurized structures like helicopters, or new generation aircraft composed of carbon sandwich primary structures, such as the "Elixir" from Elixir Aircraft (see Fig. 1), certified by the EASA in June 2020.

Most of the time, asymmetric structures are used [2–4] and, due to weight constraints, the skins can themselves be non-symmetric composite stacks.

Local buckling, called "wrinkling", is one of the main causes of failure of these light structures. It is a local instability that can occur when a real sandwich structure is subjected to compression or shear loading, which manifests itself in the form of short wavelength wrinkles in the skins, of the order of the thickness of the sandwich. Three wrinkling modes may be observed [5]: antisymmetric wrinkling, symmetric wrinkling and one-sided wrinkling (see Fig. 2).

In an industrial approach to structural design, global finite element models (GFEM) are used for pre-sizing large aeronautical structures (wings, fuselage etc.). GFEM are made with large shell elements and cannot capture wrinkling modes because of the short wavelengths involved and the 3D nature of the phenomenon. The engineer therefore needs an effective, efficient tool to prevent the occurrence of wrinkling. A methodology based on a local analytical approach, if possible, providing reliable, conservative results and validated by numerical models, needs to be developed.

Analytical wrinkling formulas have been under development since the Second World War. The simplest model is the Winkler formulation, in which the elastic response of the core is defined by springs in compression. This excludes shear deformation of the core and only one-sided or symmetric modes can be represented. Reference can be made to the books by Hetenyi [6] and Allen [5].

Then come the formulations based on an isotropic elastic foundation, where two major groups are represented. For the first group, the core is modelled as a 1-dimensional elastic medium, i.e. the core

* Corresponding author.
E-mail address: bruno.castanie@insa-toulouse.fr (B. Castanié).

https://doi.org/10.1016/j.compstruct.2021.114387

Fig. 1. The Elixir, EASA certified two-seater light aircraft (https://elixir-aircraft.com).

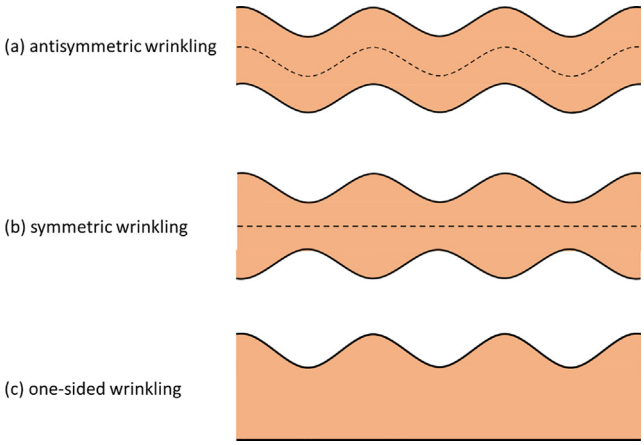

Fig. 2. The different wrinkling modes.

supports stresses only in the thickness direction, whence the name "anti-plane core stress assumption". This is the case of Hoff and Mautner's pioneering formulation [7] where the perturbation is assumed to decay linearly over the core thickness, unlike in Plantema's work [8], where the core is considered to be infinitely thick and the perturbation to decay exponentially. For the second group, the core is modelled as a 2-dimensional elastic medium. For Allen [5], then later Niu and Talreja [9], the axial stiffness of the core is retained. In this way, an isotropic core is conveniently represented, which has a mechanical response characterized by an Airy function. These pioneering formulations [7,8,5] can be expressed as:

$$\sigma_{crit} = Q\left(E_f E_c G_c\right)^{1/3} where Q is a constant$$

E_c, G_c and E_f are, respectively, the core normal modulus, the core transverse shear modulus and the skin Young's modulus. The value of constant Q varies from 0.4 to 0.9 depending on the authors (0.91 for Hoff and Mautner, 0.85 for Plantema and 0.78 for Allen). Hoff and Mautner, after a test campaign, recommend a "practical" constant Q of 0.5 [7]; in the sense that Q plays the role of a safety coefficient and masks the complex mechanics of local instabilities.

These formulations have been enriched by adding orthotropy: in the skins with Fagerberg and Zenkert [10] and in the core with Vonach and Rammerstorfer [11]. The possibility of a multiaxial loading is proposed by Sullin [12], Birman et al. [13] and summarized in Kassapoglou's book [14].

Following a different path, many authors have tried to achieve unified models capable of describing global and local modes (both symmetric and antisymmetric) to investigate the possible interactions between these different behaviours. The first work in this sense was done by Benson and Mayers [15] and taken up by Hunt [16] then by Léotoing et al. [17] with an investigation of the non-linear post-buckling behaviour [18]. Finally, Douville and le Grognec propose an analytical model that, to the authors' knowledge, is the most complete and the most recent [19]. It is also noteworthy that these approaches are based on a beam assumption although real structures are almost shells.

Other authors have chosen to be as rigorous as possible at the cost of numerical resolution. This is the case of Ji and Waas [20]. In this framework, a standardization of kinematic theories for multi-layered plates has been performed by Carrera [21]. The Carrera Unified Formulation (C.U.F.) is a compact index notation, where different kinematic models are formulated with the corresponding governing equations implemented in a single computer program. This framework has been used by D'Ottavio and Polit to provide a numerical wrinkling model [22] based on a "Layer-wise" theory, whose principle is to discretize the sandwich in several numerical layers in order to refine the model if necessary. C.U.F. has since been formally generalized to a "sublaminate" approach referred to as S.G.U.F., which allows dedicated models to be introduced for skins and the core, thus reducing the computational cost of the wrinkling model without affecting the accuracy [23,24].

These models are validated by referring to benchmark problems for which exact analytical solutions are available or Finite Element (FE) results have been obtained [19,23–25]. However, while this demonstrates a rigorous and scientific approach to performing model validation, these numerical models have not been challenged by a realistic approach. The industrial vision, i.e. the practical use of these models for pre-sizing sandwich structures against wrinkling, is not very present in the literature.

The ideal, from the design engineer's point of view, would be to define the local buckling phenomenon by an analytical formulation with as few parameters as possible. The objective of the designer is not absolute precision but the coherence of the model in various, realistic configurations. In this sense, Zenkert's sandwich construction handbook [26] and NASA's technical documents of the 1960's [12] recommend the historical formula (1) with the "practical" constant Q of 0.5, which gives the formula still massively used by manufacturers for the design of local instabilities in sandwich structures. Generally speaking, manufacturers are using Hoff and Mautner formulae with high security coefficients–up to 3, for example.

Therefore, the purpose of this paper is to provide a benchmark that can demonstrate the limits/relevance of these analytical models in an actual industrial application.

The work presented here is a comparison of the critical wrinkling loads between a realistic configuration modelled by a 3D FEM, the corresponding solutions of different analytical models in the literature, and the numerical S.G.U.F. model of D'Ottavio and Polit [23]. This numerical model is found to be situated between the analytical formulations and the FEM. In fact, the numerical model uses the same 2D stress/strain state and boundary conditions as the analytical formulations. However, its very rich, quasi-3D formulation relaxes many of the kinematic hypotheses upon which the analytical models are formulated and is hence close to the FE model. The comparison of the numerical model with the analytical formulas highlights the approximations of the kinematic assumptions, and the comparison with the 3D FEM shows the influence of the 3D stress state, as well as the boundary conditions inherent in the FEM (see Fig. 3).

With the above mentioned purpose in mind, the paper is organized as follows. Firstly, the case study is described, with the analytical, numerical, and FE models used; subsequently, the benchmark is discussed, by comparing the models with the 3D FEM and looking into correlations. Finally, some conclusions are drawn and perspectives envisaged.

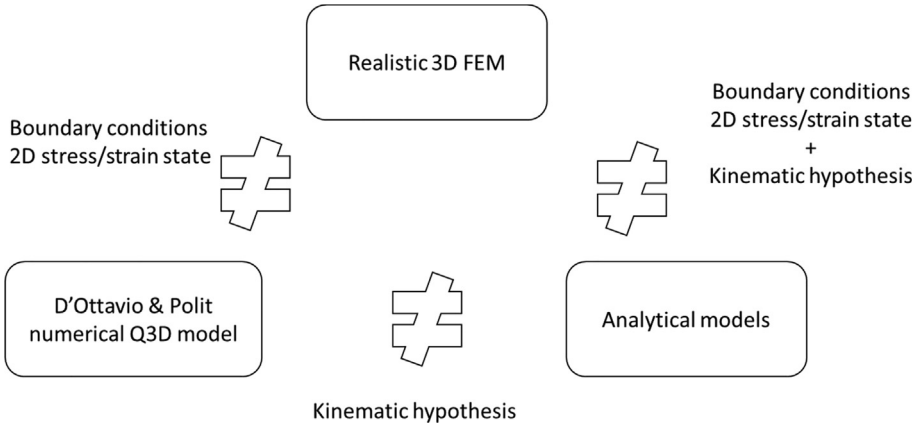

Fig. 3. Comparison scheme of the different models.

2. Case study

The case study concerns a range of sandwich composite beams subjected to uni-axial compressive loading. The sandwich structures are consistent with those used by Elixir Aircraft with orthotropic balanced carbon skins and honeycomb or foam core. The dimensions of the beam are 200 × 60 × 50 mm (see Fig. 4). Sandwich structures generally used in lightweight aircraft have thicknesses that do not exceed 10 mm, which is not respected here (thickness = 50 mm). This significant thickness is preferred to make local wrinkling modes dominant over global buckling modes.

2.1. 3D FEM reference model

The 3D framework allows reality to be approached in the sense that a 3D FEM could be used by an engineer in a test/simulation dialogue, or in a local dimensioning approach. Abaqus software is used. The mesh size is fine enough to take account of the least influence on the critical buckling load [18]. The average element size is 1 mm and at least 4 elements per half wavelength are observed in the most critical case (see Fig. 4). The types of elements used are also noted in Fig. 4.

Boundary conditions are not totally in conformity with analytical models. The analytical formulations and the numerical S.G.U.F. model are based on a periodic response over the length of the sandwich beam. This can be interpreted as an infinite medium: no boundary condition other than that formed by the trigonometric functions that define the solution is considered. In FEM, the boundary conditions always have an effect but it can be reduced if the length of the beam is sufficiently greater than the half wavelength [18]. Linear perturbation buckle computation (eigenvalue prediction) is used to define the reference buckling load.

2.2. Analytical wrinkling formulas used for the benchmark

In general, wrinkling analytical models are taken to be infinitely long skins attached to an elastic foundation (see Fig. 5). The skins and the foundation are of width b, and a plane stress/strain assumption is used in the ZX plane. A plane stress assumption can be used if b is small, or a plane strain assumption can be used if b is considered infinite. The cross-section is symmetric, i.e., $t_{tot} = t_c + 2t_s$, where t_c and t_s denote the core and skin thicknesses, respectively.

The buckling differential equation of the face supported by an elastic foundation can be written as [9]:

$$D_s \frac{d^4 w_s}{dx^4} + \frac{d}{dx}\left(P_s \frac{dw_s}{dx}\right) - b\sigma + \frac{dm}{dx} = 0$$

where D_s is the flexural rigidity of the skin, P_s is the axial compression load carried by the skin, w_s is the vertical deflection of the skins andσ is the corresponding normal stress between the face and the elas-

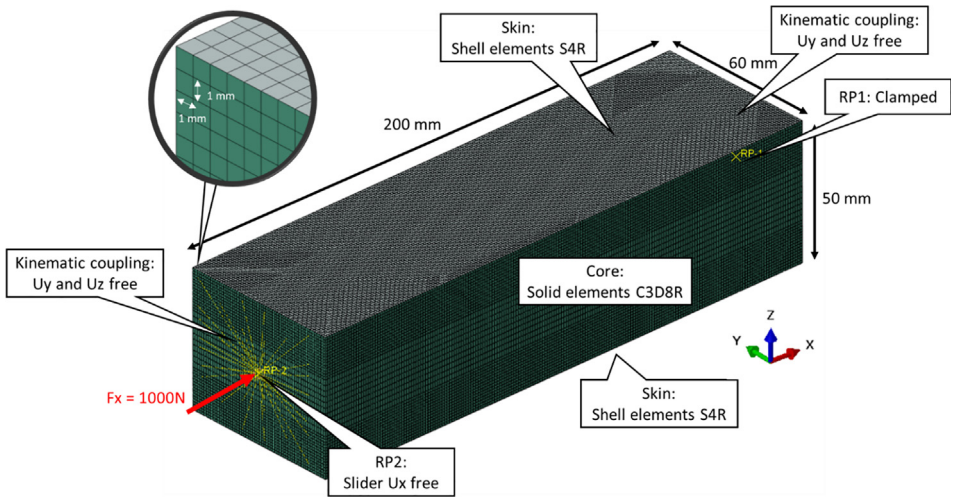

Fig. 4. 3D FEM with its boundary conditions.

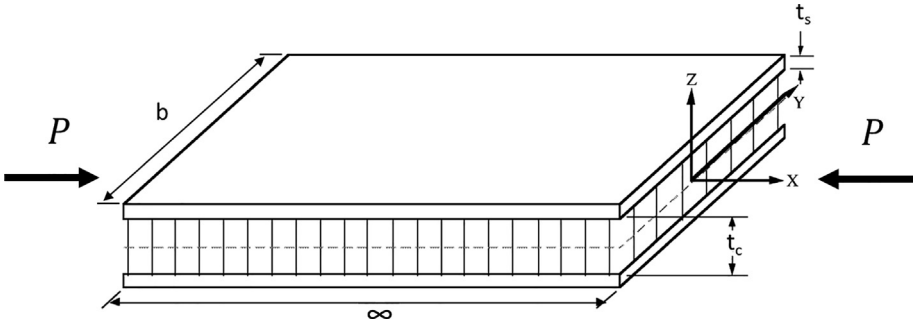

Fig. 5. Geometry of analytical models.

tic foundation. The distributed bending moment *m*is often neglected as a second order effect because of the thin face assumption [5]. Due to the huge difference of axial stiffness between the two materials, the uniaxial stresses in the precritical state are far larger in the skins than in the core. The initial stress is considered to be in the skins only. Then the skins are assumed to buckle into a trigonometric function with a half wavelength *l*.The main difference from the analytical model is the translation of normal stress σ and the propagation of the perturbation along the core thickness.

Analytical formulas are chosen in the literature in order to cover a broad panel of kinematics hypotheses. Also, attention is paid to the "usability" of the formulation from a designer's point of view. The formulation must be easily usable on an excel sheet, with few material parameters (engineering constants). A minimization with 1 variable is accepted.

A brief reminder of the main particular assumptions used in the models is given below. More details and formulas can be found in the references.

Assumptions of the models:

The Winkler formulation [27]

- Core: elastic springs of stiffness $k = \frac{E_c}{t_c/2}$.
- Skins: isotropic Euler-Bernoulli beams in pure bending.
- Solution method: direct solution of Partial Differential Equation (PDE).

Hoff & Mautner, 1945 [7]

- Core: isotropic continuum under anti-plane core stress assumption.
- Skins: isotropic Euler-Bernoulli beams in pure bending.
- Solution method: potential energy minimization.

Léotoing et al., 2002 [17]

- Core: isotropic continuum with finite thickness, the interactions between faces are retained. Transverse shear stress is linear other the core thickness.
- Skins: isotropic Euler-Bernoulli beams in pure bending.
- Solution method: linearization of PDE constructed by the Principle of Virtual Work.

Niu & Talreja, 1999 [9]

- Core: isotropic continuum with finite thickness. Stress field is expressed by Airy function in the form of a Fourier series.
- Skins: isotropic Euler-Bernoulli beams under pure bending.
- Ritz Method

Douville & Le Grognec, 2013 [19]

- Core: isotropic continuum with finite thickness.
- Skins: isotropic Euler-Bernoulli beams in pure bending.
- Solution method: Differential equations obtained from a general bifurcation in a 3D framework then restrained in a 2 dimensional framework to obtain an analytical formula.

3. Plane strain assumption

The plane strain assumption is more coherent for the comparison with a 3D FEM. Because the width b is not negligible, the plane strain assumption is thus taken for the analysis. To pass from plane stress assumption to plane strain assumption, the Young's modulus and Poisson's ratio are modified such that:

$$E \rightarrow \frac{E}{(1-\nu^2)} and \nu \rightarrow \frac{\nu}{(1-\nu)}$$

4. Composite laminated skins

Composite laminated skins are studied, and the use of the flexural rigidity D_f in the direction of the compressive load is recommended instead of the membrane rigidity E_f.

The flexural rigidity of the laminate is defined as:

$$D_f = \frac{12}{D_{11}^* t_f^3}$$

The flexural orthotropic Poisson's ratios are defined as:

$$\nu_{fxy} = -\frac{D_{12}^*}{D_{11}^*} and the inverse \nu_{fyx} = -\frac{D_{12}^*}{D_{22}^*}$$

where the Matrix D^* is the inverse of the **bending stiffness matrix of the laminate.** If the coupling terms between curvature and in-plane strains (matrix) is not zero, which is the case for asymmetric laminates, the bending stiffness calculated, D_f, do not consider this coupling and will be erroneous (see discussions on stacking with asymmetric skins).

4.1. Quasi-3D SGUF model

The bifurcation buckling problem is stated in weak form expressing the stability of a linear elastic body in the *x-z* plane subjected to an axial initial stress σ_{xx}^0 [35]:

$$\int_L \int_{t_{tot}} \left[\delta\varepsilon_{xx}\left(C_{11}\varepsilon_{xx} + C_{13}\varepsilon_{zz}\right) + \delta\varepsilon_{zz}\left(C_{13}\varepsilon_{xx} + C_{33}\varepsilon_{zz}\right) + \delta\gamma_{xz}C_{55}\gamma_{xz} + \delta u_{x,x}\left(\lambda\sigma_{xx}^0 u_{x,x}\right) + \delta u_{z,x}\left(\lambda\sigma_{xx}^0 u_{z,x}\right)\right] dz dx = 0 \quad (1)$$

where the critical buckling load is defined by the scalar parameter λ that multiplies the initial stress characterizing the initial equilibrium condition. The perturbation strains are defined by the usual linearized geometric relations $\varepsilon_{xx} = u_{x,x}$, $\varepsilon_{zz} = u_{z,z}$, $\gamma_{xz} = u_{x,z} + u_{z,x}$.

The initial stress σ_{xx}^0 is defined in terms of a uniform axial strain ε_{xx}^0 produced by an end shortening of the whole sandwich strut. Therefore,

the initial stress is constant across each ply but is non-uniform across the sandwich cross-section as it depends on the stiffness of the ply (p), see also [24]:

$$\sigma_{xx}^{0(p)} = Q_{11}^{(p)}\varepsilon_{xx}^{0} \text{with} Q_{11}^{(p)} = C_{11}^{(p)} - \frac{C_{13}^{(p)}C_{31}^{(p)}}{C_{33}^{(p)}} \tag{2}$$

The total axial load per unit width is obtained as the sum of all ply-wise stresses:

$$P = \int_{h_{tot}} \sigma_{xx}^{0(p)} \mathrm{d}z = \varepsilon_{xx}^{0} \int_{h_{tot}} Q_{11}^{(p)} \mathrm{d}z = A_{11}\varepsilon_{xx}^{0} \tag{3}$$

The stiffness coefficients C_{pq} with p; q $\in$ {1; 3; 5} in Eqs. (1) and (2) are kept constant during the perturbation from the initially stressed state. In a plane strain setting ($\varepsilon_{yy} = 0$), these coefficients are the usual stiffnesses defining the 3D generalized Hooke law ($C_{pq} = C_{pq}$), whereas they are the reduced stiffnesses $C_{pq} = C_{pq} - \frac{C_{p2}C_{2p}}{C_{22}}$ if a plane stress setting is employed ($\sigma_{yy} = 0$). The weak form Eq. (1) allows the a priori assumptions to be introduced for the displacement field that describes the perturbed (buckled) shape across the thickness t_{tot} of the sandwich strut. These are formulated according to the S.G.U.F. approach as a Layer-Wise (LW) assembly of $N_L = 3$ sublaminates representing the 2 skins and the core, where an arbitrary model expressed in Unified Formulation is adopted for each sublaminate, see [36] for more details. The resulting approximation is thus expressed as

$$u_x(x,z) = \bigcup_{k=1}^{3} \sum_{\tau=0}^{N_{bx}^k} F_\tau^k(z_k)\widehat{u}_\tau(x); u_z(x,z) = \bigcup_{k=1}^{3} \sum_{\tau=0}^{N_{bz}^k} F_\tau^k(z_k)\widehat{w}_\tau(x) \tag{4}$$

where F_τ^k are the thickness functions used in the k^{th} sublaminate and expressed in function of its local coordinate z_k. The present Quasi-3D (Q3D) model adopts a higher-order Layer-Wise (LW) description for providing reference results:

- $LD_{3;2}$ for the skin laminates: the axial displacement $u_x(z)$ is cubic and the out-of-plane displacement, $u_z(z)$, quadratic in each ply.
- $ED_{12;12}$ for the core: the axial and out-of-plane displacements $u_x(z)$ and $u_z(z)$ are represented by a 12th order polynomial.

The thickness functions are introduced into Eq. (1); the derivatives and integration along z are carried out explicitly and the following arrays are computed upon cycling over all indices $\tau,\rho \in [0,N^k]$ and assembling all ply-wise (superscript (p)) contributions for all sublaminates (superscript k):

$$\{Z_{uu11}^{\tau\rho}; Z_{uw13}^{\tau\rho,\tau z}; Z_{ww33}^{\tau z,\rho z}\} = \bigcup_{k=1}^{3} \int_{h_k} \left\{C_{11}^{(p)}F_{u_\tau}^k F_{u_\rho}^k; C_{13}^{(p)}F_{u_\tau}^k F_{w_{\rho,z}}^k; C_{33}^{(p)}F_{w_{\tau,z}}^k F_{w_{\rho,z}}^k\right\}\mathrm{d}z_k \tag{5a}$$

$$\{Z_{uu55}^{\tau,z\rho,z}; Z_{uw55}^{\tau,z\rho}; Z_{ww55}^{\tau\rho}\} = \bigcup_{k=1}^{3} \int_{h_k} C_{55}^{(p)}\left\{F_{u_{\tau,z}}^k F_{u_{\rho,z}}^k; F_{u_{\tau,z}}^k F_{w_\rho}^k; F_{w_\tau}^k F_{w_\rho}^k\right\}\mathrm{d}z_k \tag{5b}$$

$$\left\{Z_{G_{uu}}^{\tau\rho}; Z_{G_{ww}}^{\tau\rho}\right\} = \bigcup_{k=1}^{3} \int_{h_k} Q_{11}^{(p)}\left\{F_{u_\tau}^k F_{u_\rho}^k; F_{w_\tau}^k F_{w_\rho}^k\right\}\mathrm{d}z_k \tag{5c}$$

These arrays correspond to the model adopted for the sandwich stack and include the linear stiffness contributions, Z, and the "geometric" stiffness contributions, Z_G. Contrary to the FEM and in analogy to the analytical models presented in Section 2.2, this model adopts a strong-form solution along the coordinate x; the local stability equations in the domain $\times \in [0, L]$ and the required boundary conditions are hence obtained upon applying the divergence theorem to the terms whose virtual variations are derived with respect to x. The solution is defined in terms of trigonometric functions as

$$\widehat{u}_\tau(x) = U_\tau \cos\left(\frac{\pi x}{L_x}\right); \widehat{w}_\tau(x) = W_\tau \sin\left(\frac{\pi x}{L_x}\right) \tag{6}$$

where $L_x = L/m$ is the half-wavelength of the periodic response. This Navier type solution exactly verifies the essential boundary conditions $u_3(x = 0, L) = 0$ as well as the natural condition $\sigma_{xx}^p(x = 0; L) = 0$, stating that the external initial load $\sigma^{0(p)}$ remains constant throughout the perturbation. The linearized stability equation is eventually cast in the conventional eigenvalue problem for a given half-wavelength $L_x(m)$:

$$\begin{bmatrix}\boldsymbol{U}\\ \boldsymbol{W}\end{bmatrix}_m^{\mathrm{T}} \left(\begin{bmatrix}\boldsymbol{K}_{UU} & \boldsymbol{K}_{UW}\\ \boldsymbol{K}_{UW}^{\mathrm{T}} & \boldsymbol{K}_{WW}\end{bmatrix}_m + \lambda_m \begin{bmatrix}\boldsymbol{K}_{GUU} & 0\\ 0 & \boldsymbol{K}_{GWW}\end{bmatrix}_m\right)\begin{bmatrix}\boldsymbol{U}\\ \boldsymbol{W}\end{bmatrix}_m = \begin{bmatrix}0\\ 0\end{bmatrix} \tag{7}$$

whose solution provides the through-thickness modes $[\mathbf{U};\mathbf{W}]^{\mathrm{T}}$ corresponding to the half-wavelength $L_x = L/m$ and the associated scalar parameters λ_m that define the critical loads $P_{cr}(m) = \lambda_m P$ according to Eq. (3). The buckling/wrinkling load is then found as the lowest critical load among all possible wavelengths:

$$P = \min_m (P_{cr}(m)) at m = m^*, L_x^* = L_x(m^*) = \frac{L}{m^*} \tag{8}$$

4.2. Cases studied

4.2.1. Materials used:

The properties of the materials used are industrial standards and are proposed in Table 1.Table 2.

4.2.2. Stacking used:

Asymmetry is one of the characteristics of the sandwich skins used in light aviation. An asymmetry parameter φ is defined from the position of the skin's neutral fibre (see Fig. 6):

$$\varphi = \frac{c}{a} with c = -\frac{B_{11}^*}{D_{11}^*}$$

The position of neutral fibre in the skin is defined by $M_x(z) = \varepsilon_x(z) = 0$; where $M_x(z)$ and $\varepsilon_x(z)$ are respectively the bending moment and the axial deformation along the skin thickness. A negative value of φ means that the neutral fiber is moved inwards, i.e. in the direction of the core of the sandwich.

Six sandwich stacking sequences are studied.

The ST-0 stacking acts as a control configuration with symmetrical skins and a homogeneous core. Then comes the more "technological" stacking that can be found in a lightweight aircraft structure, with asymmetric skins (ST-1; ST-3) and an orthotropic Honeycomb core (ST-2). Then a stacking sequence is defined with a large proportion of UniDirectional plies that can take up a large part of the longitudinal force (ST-4) and, finally, a stacking with a single ply (ST-5) is used.

5. Results and discussion

5.1. Wrinkling modes computed by the FEM

Niu & Talreja, Léotoing et al., and Douville & Le Grognec demonstrate that the critical stress for asymmetric wrinkling is always the lowest when the core is isotropic. However, when the skins are thin with respect to the core thickness, the loads leading to asymmetric and symmetric modes are almost equal, which is the case for this study case (see Fig. 7).

It can be noticed that, for the stacking with orthotropic honeycomb core (ST-2), the symmetrical mode is preponderant. This phenomenon has been reported by several authors [28,11,22]. D'Ottavio and Polit explain that "in case of high orthotropy as honeycomb core, when axial modulus is nearly equal to zero, the contribution of the transverse shear energy gets negligible for the symmetric mode which

Table 1
Material properties used for the case study.

	E_1 (Mpa)	E_2 (Mpa)	E_3 (Mpa)	G_{12} (Mpa)	G_{13} (Mpa)	G_{23} (Mpa)	ν_{12}	ν_{13}	ν_{23}	Ply thickness (mm)
Fabric	55000	55000	10000	4000	4000	4000	0.04	0.3	0.3	0.2
UniDir	120000	10000	10000	4000	4000	3333	0.3	0.3	0.5	0.16
FOAM	50	50	50	30	30	30	0.3	0.3	0.3	
Nomex Honeycomb	0.5	0.5	140	1	40	25	0.9	0.01	0.01	

Table 2
Definition of the 6 sandwich stacking sequences.

	ST-0	ST-1	ST-2	ST-3	ST-4	ST-5
Stacking	Fabric +/ 45°	Fabric +/ 45°	Fabric +/ 45°	Fabric +/ 45°	Fabric +/ 45°	
	UniDir 0°	UniDir 0°	UniDir 0°		4XUniDir 0°	
	Fabric +/ 45°	Fabric 0°/90°	Fabric +/ 45°	Fabric 0°/90°	Fabric 0°/90°	Fabric 0°/90°
	Foam	Foam	Honeycomb	Foam	Foam	Foam
	Fabric +/ 45°	Fabric 0°/90°	Fabric +/ 45°	Fabric 0°/90°	Fabric 0°/90°	Fabric 0°/90°
	UniDir 0°	UniDir 0°	UniDir 0°		4XUniDir 0°	
	Fabric +/ 45°	Fabric +/ 45°	Fabric +/ 45°	Fabric +/ 45°	Fabric +/ 45°	
Skin thickness (mm)	0.6	0.6	0.6	0.44	1.08	0.22
φ	0%	-16%	0%	-28%	-8%	0%

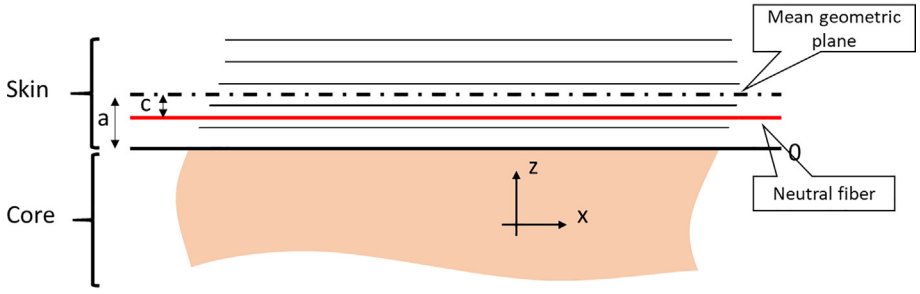

Fig. 6. Definition of the asymmetry parameter φ.

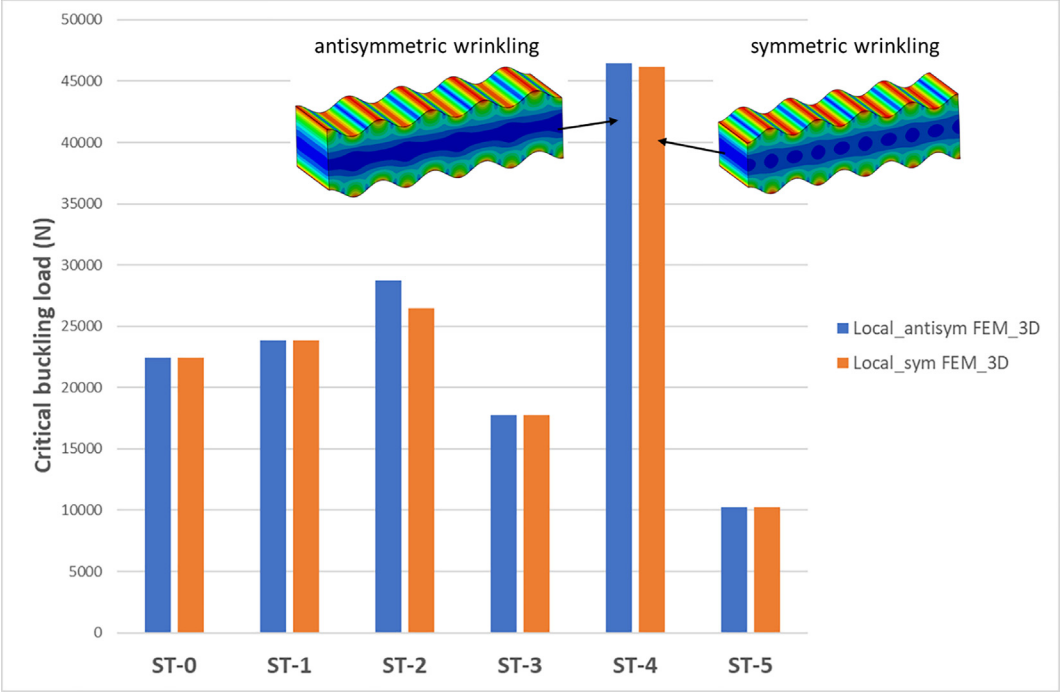

Fig. 7. 3D FEM critical local buckling load for antisymmetric and symmetric modes.

becomes preponderant whereas antisymmetric wrinkling mode is indeed always associated with a transverse shear deformation of the core." As the symmetric mode shows a lower buckling load, only this mode will be compared with the results of the analytical models.

5.2. "Radar" type comparison graphs

"Radar" type comparison graphs were chosen to illustrate comparisons between the models. The different models are listed and presented in relation to the relative percentage gap between the buckling loads of the models and that of the FEM. The dotted line seen in the different graphs indicates perfect correlation with the FEM.

5.2.1. Homogeneous foam core

For the ST-0 sandwich stacking (see Fig. 8), the Winkler formulation does not match the FEM because it totally neglects shear stress in the core, unlike the FEM, which models a continuum of quasi-isotropic medium.

Léotoing et al.'s model shows poor correlation. According to the authors, the difference between analytical and numerical results can be partly explained by the simplistic analytical shear stress distribution (linear through the core thickness), which does not estimate the actual energy contribution of the shear stress accurately [29].

Niu & Talreja, like Douville & Le Grognec, use an isotropic core formation. In the FEM, the foam is slightly non-isotropic in the sense that the modulus E, the shear modulus G and the Poisson coefficient ν are not linked with the Lamé formulation: $G = \frac{E}{2(1+\nu)}$. In their models, only the core modulus with Poisson coefficient is expressed; the core shear modulus comes from Lamé's formulation and should be 19.7 MPa instead of the 30 MPa introduced in the FEM. Thus, in this case, the models are conservative, which is interesting from an engineering point of view. Unlike Hoff's model with the theoretical coefficient. The model with "practical" coefficient $Q = 0.5$, is very conservative compared to the FEM. This "abatement" comes from test observations with their inherent aspects, boundary conditions, and defects [7], whereas the FEM is a perfect framework.

5.2.2. Orthotropic honeycomb core

For the ST-2 sandwich stacking (see Fig. 9), all the analytical models give poor results, which is quite understandable for Hoff and Mautner, Niu & Talreja, Léotoing et al., and Douville & le Grognec, because these models are constructed around a continuum isotropic core.

The Winkler model, neglecting the transverse shear of the core, should be more coherent for sandwich with honeycomb, because the axial honeycomb modulus is very low, so the contribution of the transverse shear energy becomes smaller. That is why it is suitable for the design of sandwich structures with honeycomb core according to a recent NASA technical memorandum [30]. However, in the present case, it shows bad correlation. D'Ottavio and Polit had shown the influence of the out-of-plane core orthotropy ratio $X = E_x/E_z$on the wrinkling buckling load [22]. It appears that the contribution of the transverse shear energy becomes negligible when the ratio is of the order of $X = 10^{-4}$, as the Winkler formulation correlates well for this type of ratio. However, in the case of the properties of the materials studied here (see Table 1), its value is close to $X = 7 * 10^{-3}$ and the transverse shear stress becomes non-negligible. The in-plane properties of honeycomb are not given by the suppliers, nor by the data bases (MIL-HDBK-23 [31] or NCAMP). A value of 1 MPa is often used by the engineers as the honeycomb axial stiffness. That said, it is understandable why this model is always used in an industrial setting: neglecting the transverse shear limits the critical buckling load and it is conservative.

5.2.3. Asymmetric skins

In Fig. 10, the results of the ST-0, ST-1 and ST-3 sandwich stacking are summed up. We recall that the coupling terms of a laminated skin rigidity matrix are non-zero in cases of asymmetric skin, and are not considered in the flexural rigidity of the laminated skin. Surprisingly, the stacking sequences with asymmetric skins (ST-1; ST-3) demonstrate a similar level of correlation compared to the symmetric skin stacking (ST-0), which shows that, for asymmetric skins, up to 28% offset of the neutral fibre from the mean plane geometry, the flexural/membrane coupling is not prevalent in the critical buckling load.

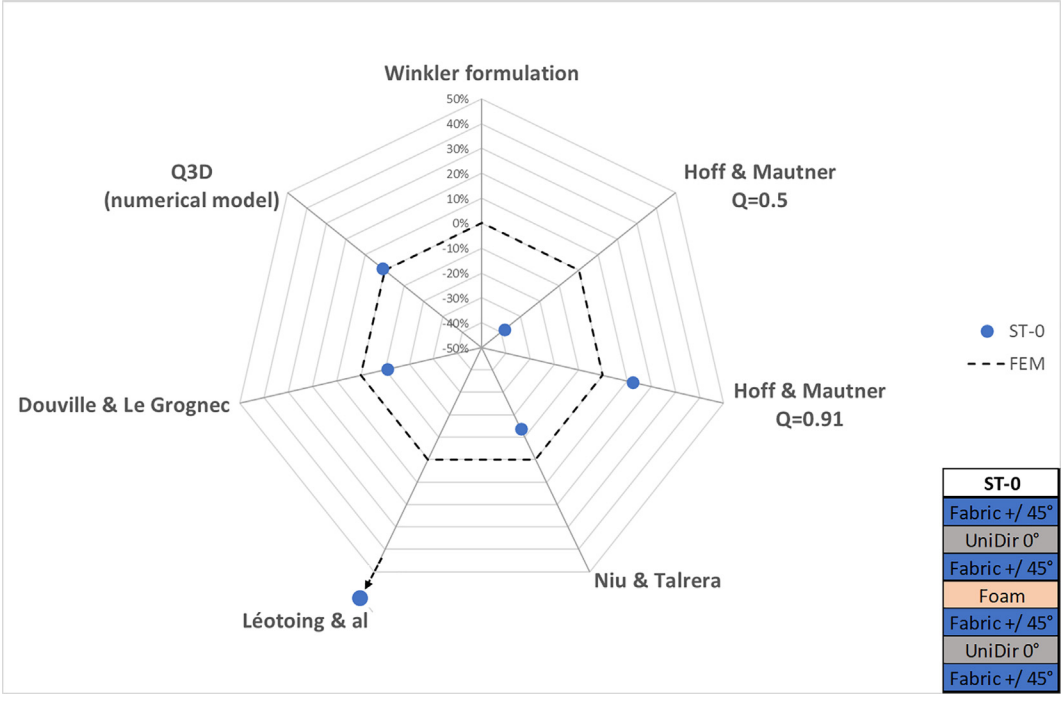

Fig. 8. Radar type comparison graph for ST-0 sandwich stacking: symmetric balanced orthotropic skin with foam core.

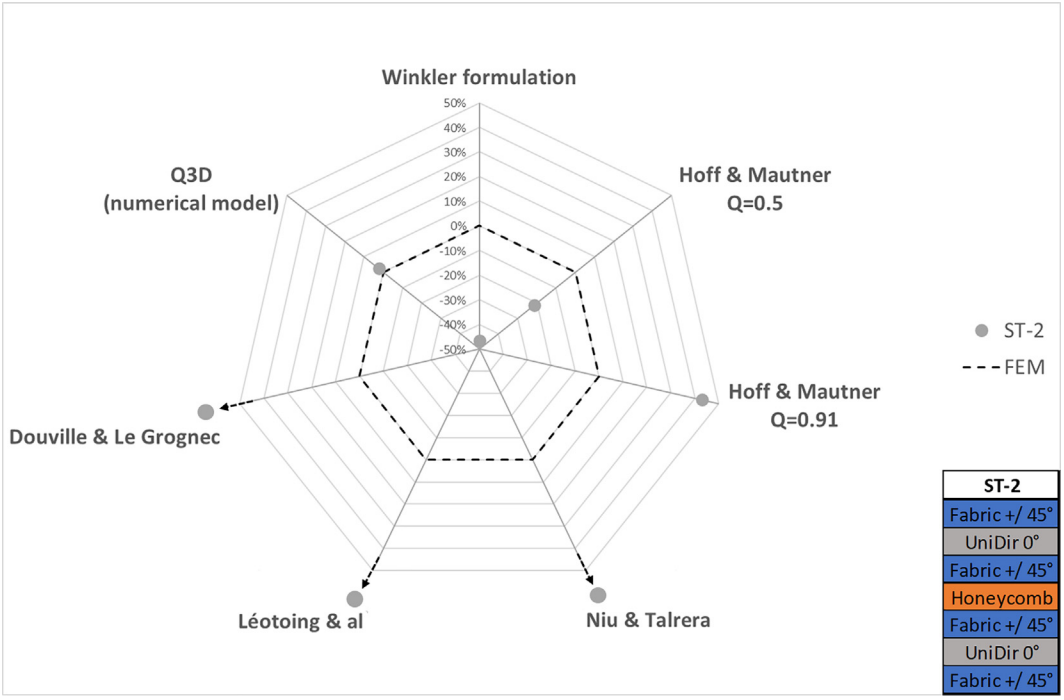

Fig. 9. Radar type comparison graph for ST-2 sandwich stacking: Symmetric balanced orthotropic skin with honeycomb core.

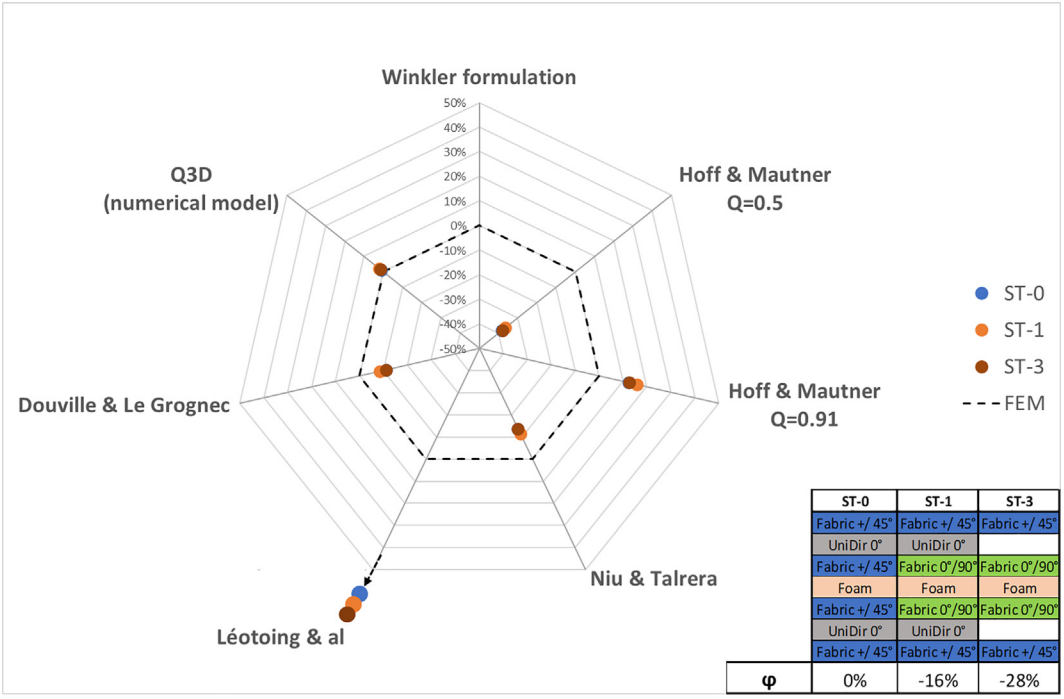

Fig. 10. Radar type comparison graph for symmetric skins (ST-0) and asymmetric skin (ST-1; ST-3).

5.2.4. UD dominated stacking in skin

The stacking sequence ST-4, with a high proportion of UD 0° ply, shows correlation similar to that of the ST-0 stacking sequence (see Fig. 11). The improvement of Léotoing et al.'s model can be explained by a longer buckling wavelength with the increase of the skin thickness and modulus. The influence of transverse shear, which is the limitation of this model, is less marked than for the case with short wavelength [9].

5.2.5. A single ply in skin

In the analytical models studied, the core does not take up any axial load and the critical buckling load is computed as $P_{crit} = \sigma_{crit} * 2 * b * t_f$. In the ST-5 stacking sequence, the core takes up about 9% of the total load applied to the sandwich beam. This explains why the correlation of the analytical models, for a stacking sequence with a very small skin thickness, is less, in absolute value, than for a configuration with a thicker skin (see Fig. 12). The hypoth-

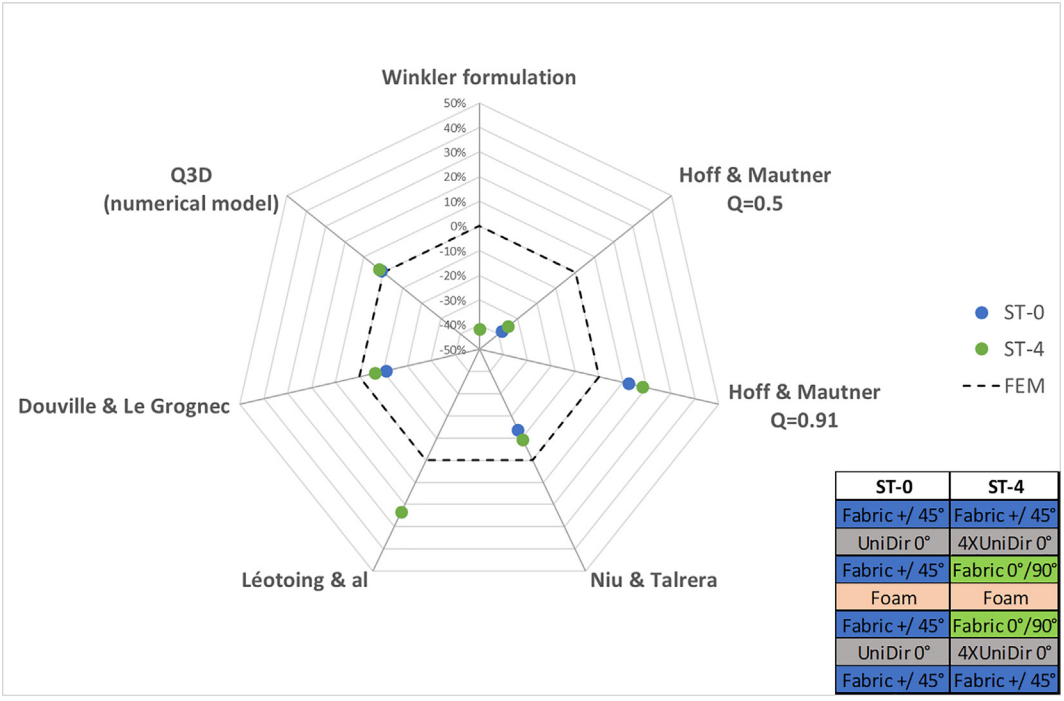

Fig. 11. Radar type comparison graph for ST-0 and ST-4 with a large proportion of UniDirectional ply.

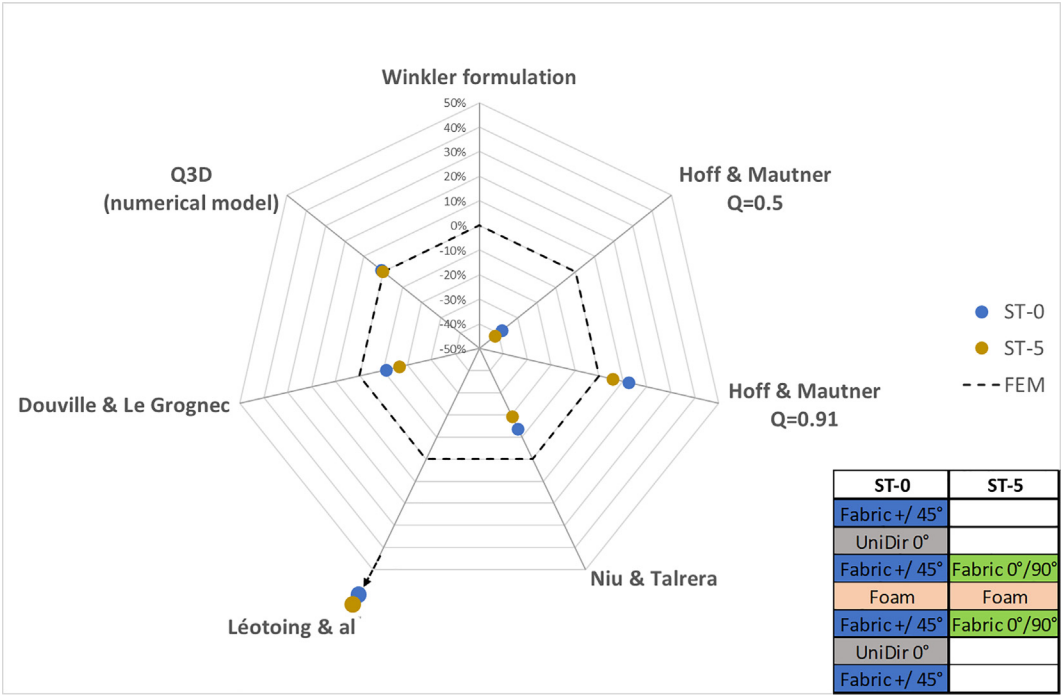

Fig. 12. Radar type comparison graph for ST-0 and ST-5 with a single ply.

esis that the skins take up the totality of the pre-critical axial load is conservative and thus interesting from the engineering point of view.

6. Conclusions

This paper presents a benchmark of analytical wrinkling formulas compared to a 3D finite Elements Model. The study case is a sandwich composite beam subjected to uniaxial compressive loading with stacking sequences and material properties (orthotropic balanced carbon skins and honeycomb or foam cores) in accordance with an industrial application in light aviation. These analytical models are challenged under a framework (3D stress state; orthotropy; skin asymmetry) far from the assumptions on which the analytical formulations were based. The paper shows how the analytical solutions behave compared to a realistic 3D FEM, and the conclusions can be summarized as follows:

- The symmetrical mode is the predominant wrinkling mode for honeycomb core stacking, as already observed in the literature [28,11,22].
- Hoff and Mautner's formula with the practical constant $Q = 0.5$ is conservative for all sandwich stacking sequences, sometimes up to -50%, and an interesting conservative correlation is observed for honeycomb core stacking (around -20%)
- The models by Niu & Talreja and Douville & Le Grognec show an interesting conservative correlation for foam core configurations (between -10% and -20%). On the other hand, they are unusable (too optimistic) for sandwich beams with honeycomb core. The isotropic continuum core hypothesis is too far from the honeycomb mechanical characteristic.
- The Winkler formulation, which is used for the design of sandwich structures with honeycomb core [30], is too conservative for the honeycomb core stacking studied, because the out-of-plane orthotropy ratio ($X = E_x/E_z$) chosen is too high to allow the transverse shear energy to be neglected.

For foam core stacks, the formulation is unusable because the compressive spring foundation is too far from the foam continuum medium.

- The asymmetric skins studied had little influence on the wrinkling load.
- In the case of very thin skins with high core thickness, the core takes up a non-negligible part of the total load applied to the sandwich beam, which is not considered in the analytical buckling load computations. Nevertheless, this assumption remains conservative.
- This study shows that classical analytical formulations are not suitable for recent advanced sandwich structures and generate overconservative or unreliable results.
- The Q3D SGUF numerical model shows a quasi-perfect correlation with the FEM for all sandwich stacking sequences studied. The plane strain assumption used in this model is good enough to represent the 3D sandwich beam subjected to compressive uniaxial load that was considered. This most advanced formulation, of the C.U.F. formulation class, is the only one that should be implemented in a python routine in a GFEM and can be considered for the design of actual lightweight aeronautical structures. Its reliability can permit the currently used security coefficient to be diminished.

This study has some limitations, which bring perspectives. First, the case study imposes a considerable core thickness (50 mm), which means that the skins' interaction mechanisms are ignored. This is not the case for a sandwich structure used in light aviation, where the core thickness is around 10 mm. Secondly, the analytical model is evaluated in a perfect framework. However, it is known that the wrinkling phenomenon is sensitive to boundary conditions and defects–hence the great difficulty of correlation between experiments and analytical models [32–34]–and few wrinkling test campaigns are available in the literature. For a full evaluation, an experimental test/-analytical models dialogue needs to be completed. Finally, uniaxial compressive load is a particular loading case and sandwich structures are often subject to multiaxial load. The stability problem of sandwich structures under combined loads arises. Several authors have been worked on this subject [12–14] bringing analytical solutions and a benchmark of the same philosophy that proposed in this paper, should interesting to be done.

Declaration of Competing Interest

The authors declare that they have no known competing financial interests or personal relationships that could have appeared to influence the work reported in this paper.

Acknowledgment

The authors dedicate this work to Prof. Erasmo Carrera for his lifelong contribution to stimulating the advances in the mechanics of composite structures.

References

[1] Castanie B, Bouvet C, Ginot M. Review of composite sandwich structure in aeronautic applications. Comp Part C Open Access 2020;1:100004. https://doi.org/10.1016/j.jcomc.2020.100004.
[2] Castanié B, Barrau J-J, Jaouen JP. Theoretical and experimental analysis of asymmetric sandwich structures. Comp Struct 2002;55:295–306. https://doi.org/10.1016/S0263-8223(01)00156-8.
[3] Fink A, Einsmann C. Discrete tailored asymmetric sandwich structures. Comp Struct 2020;238:. https://doi.org/10.1016/j.compstruct.2020.111990111990.
[4] Rion J, Leterrier Y, Månson J-A, Blairon J-M. Ultra-light asymmetric photovoltaic sandwich structures. Comp Part A 2009;40(8):1167–73. https://doi.org/10.1016/j.compositesa.2009.05.015.
[5] Allen HG. In: Analysis and Design of Structural Sandwich Panels. Elsevier; 1969. p. 156–89. https://doi.org/10.1016/B978-0-08-012870-2.50012-2.
[6] Hetenyi M. Beams on Elastic Foundation Theory. The University of Michigan Press; 1946.
[7] Hoff NJ, Mautner SE. The buckling of sandwich type model. J Aeronaut Sci July 1945;12. https://doi.org/10.2514/8.11246.
[8] Plantema FJ. Sandwich Construction: The bending and buckling of sandwich beams. Plates and Shells 1966.
[9] Niu K, Talreja R. Modeling of wrinkling in sandwich panels under compression. J Eng Mech 1999;125(8):875–83. https://doi.org/10.1061/(ASCE)0733-9399(1999)125:8(875).
[10] Fagerberg L, Zenkert D. Effects of anisotropy and multiaxial loading on the wrinkling of sandwich panels. J Sand Struct Mater 2005;7:177–94. https://doi.org/10.1177/109963205048525.
[11] Vonach WK, Rammerstorfer FG. Wrinkling of thick orthotropic sandwich plates under general loading conditions. Arch Appl Mech 2000;70(5):338–48. https://doi.org/10.1007/s004199900065.
[12] Sullins RT, Smith GW, Spier EE. Manual for structural stability analysis of sandwich plates and shells. NASA Contract Reports 1969;no:CR-1457.
[13] Birman V, Bert CW. Wrinkling of composite-facing sandwich panels under biaxial loading. J Sandw Struct Mater 2004;6(3):217–37. https://doi.org/10.1177/1099636204033643.
[14] Kassapoglou C. Design and Analysis of Composites Structures. Wiley; 2010.
[15] Benson AS, Mayers J. General instability and face wrinkling of sandwich plates-unified theory and applications. AIAA J 1967;5(4):729–39.
[16] G. W. Hunt, L. S. D. Silva, G. M. E. Manzocchi. Interactive Buckling in Sandwich Structures. Proc. R. Soc. A Math. Phys. Eng. Sci. 417(1852) (1988) pp. 155–177, doi: 10.1098/rspa.1988.0055.
[17] Léotoing L, Drapier S, Vautrin A. First applications of a novel unified model for global and local buckling of sandwich columns. Eur J Mech, A/Solids 2002;21(4):683–701. https://doi.org/10.1016/S0997-7538(02)01229-9.
[18] Léotoing L, Drapier S, Vautrin A. Nonlinear interaction of geometrical and material properties in sandwich beam instabilities. Int J Solids Struct 2002;39(13–14):3717–39. https://doi.org/10.1016/S0020-7683(02)00181-6.
[19] Douville MA, Le Grognec P. Exact analytical solutions for the local and global buckling of sandwich beam-columns under various loadings. Int J Solids Struct 2013;50(16–17):2597–609. https://doi.org/10.1016/j.ijsolstr.2013.04.013.
[20] Ji W, Waas AM. Accurate buckling load calculations of a thick orthotropic sandwich panel. Compos Sci Technol 2012;72(10):1134–9. https://doi.org/10.1016/j.compscitech.2012.02.020.
[21] Carrera E, Brischetto S. A survey with numerical assessment of classical and refined theories for the analysis of sandwich plates. Appl Mech Rev 2009;62(1):1–17. https://doi.org/10.1115/1.3013824.
[22] Carrera E, Cinefra M, Petrolo M, Zappino E. Finite Element Analysis of Structures through Unified Formulation. Ltd: John Wiley & Sons; 2014.
[23] D'Ottavio M, Polit O. Linearized global and local buckling analysis of sandwich struts with a refined quasi-3D model. Acta Mech 2015;226(1):81–101. https://doi.org/10.1007/s00707-014-1169-2.
[24] Ji W, Waas AM. 2D elastic analysis of the sandwich panel buckling problem: Benchmark solutions and accurate finite element formulations. Zeitschrift fur Angew Math und Phys 2010;61(5):897–917. https://doi.org/10.1007/s00033-009-0041-z.
[25] D'Ottavio M, Polit O, Ji W, Waas AM. Benchmark solutions and assessment of variable kinematics models for global and local buckling of sandwich struts. Comp Struct 2016;156:125–34. https://doi.org/10.1016/j.compstruct.2016.01.019.
[26] Vescovini R, D'Ottavio M, Dozio L, Polit O. Buckling and wrinkling of anisotropic sandwich plates. Int J Eng Sci 2018;130:136–56. https://doi.org/10.1016/j.ijengsci.2018.05.010.
[27] D. Zenkert, The handbook of the sandwich construction. 1995.
[28] Carlsson L, Kardomateas G. Structural and Failure Mechanics of Sandwich Composites. Solid Mech Appl 2011.
[29] Hwang SF. The buckling of an orthotropic layer on a half-space. Int J Mech Sci 1998;40(7):711–21. https://doi.org/10.1016/S0020-7403(97)00122-7.
[30] Léotoing L, Drapier S, Vautrin A. Using new closed-form solutions to set up design rules and numerical investigations for global and local buckling of sandwich

beams. J Sandw Struct Mater 2004;6(3):263–89. https://doi.org/10.1177/1099636204034632.
[31] B. F. Zalewski, W. B. Dial, B. A. Bednarcyk. Methods for Assessing Honeycomb Sandwich Panel Wrinkling Failures October 2012. NASA/TM—2012-217697 October, 2012.
[32] Sandwich Construction, Military Handbook, MIL-HDBK-23.
[33] Norris CB. Short-column compressive cf strength of sandwich constructions as affected by size of cells of honeycomb core materials. US *Forest Service Resaerch Note* 1964.
[34] Ley RP, Lin W, Mbanefo U. Facesheet wrinkling in sandwich structures. NASA CR-1999-20..
[35] Fagerberg L, Zenkert D. Imperfection-induced wrinkling material failure in sandwich panels. J Sandw Struct Mater 2005;7(3):195–219. https://doi.org/10.1177/1099636205048526.
[36] D'Ottavio M, Carrera E. Variable-kinematics approach for linearized buckling analysis of laminated plates and shells. AIAA J 2010;48(9):1987–96. https://doi.org/10.2514/1.J050203.